Neuromol Med (2013) 15:82–94
DOI 10.1007/s12017-012-8197-7

ORIGINAL PAPER

Hypobaric Hypoxia and Reoxygenation Induce Proteomic Profile Changes in the Rat Brain Cortex

Raquel Hernández · Santos Blanco · Juan Peragón · Juan Á. Pedrosa · María Á. Peinado

Received: 13 July 2012 / Accepted: 24 August 2012 / Published online: 8 September 2012

Abstract Brain, due to its high metabolism, is severely affected by hypoxia/reoxygenation. In this study, cerebral cortexes from rats subjected to hypobaric hypoxia followed by several reoxygenation periods (0 h, 24 h, and 5 days) were compared with normobaric normoxic controls to identify protein-expression differences using proteomic approaches. Only 2-fold differences in spot abundance between controls and experimental groups from each reoxygenation period were considered. The proteins identified were grouped into categories, according to their similarity in function or to their involvement in the same metabolic pathway. We distinguished five groups: (1) glycolysis, including γ-enolase (NSE), and glyceraldehyde 3-phosphate dehydrogenase (GAPDH); (2) tricarboxylic acid cycle, such as aconitate hydratase (ACO2); (3) oxidative phosphorylation, like F1-ATPase chains α and β; (4) cytoskeletal, including Spna2, α-tubulin, β-tubulin, β-actin, and microtubule-associated protein RP/EB family member 3 (EB3); and (5) chaperones, like heat-shock protein 72 kDa (HSP72). NSE was upregulated while GAPDH was downregulated, both peaking at 5 days post-hypoxia. ACO2 and F1-ATPase decreased in all the reoxygenation periods. Spna2 and EB3 were expressed neither in control nor at 0 h, but 5 days post-hypoxia new expression took place. The α- and β-tubulin levels significantly fell at 0 h, but after 24 h strongly increased. Also, β-actin and HSP72 were downregulated, and the last one reached the lowest level at 24 h of reoxygenation. We conclude that the molecular mechanisms underlying hypoxia/reoxygenation in the rat cortex might consist of a close relationship between energy metabolism, cytoskeleton, and chaperones. These findings may shed light on therapeutic targets against hypoxia-related damage.

Keywords Hypoxia · Reoxygenation · Proteomics · Brain cortex · Energy metabolism · Cytoskeleton

Abbreviations

HIF-1	Hypoxia inducible factor 1
Spna2	Non-erythroid α-spectrin 2
ACO2	Aconitate hydratase
HSP72	Heat-shock protein 72 kDa
NSE	γ-enolase
GAPDH	Glyceraldehyde 3-phosphate dehydrogenase
MAPR3/EB3	Microtubule-associated protein RP/EB family member 3

Introduction

The decrease in oxygen partial pressure in tissues, organs, or systems is known as hypoxia. An insufficient oxygen supply is critical in the pathogenesis of different illnesses such as cerebral thromboembolism, heart attack, or chronic lung pathologies. There are several types of hypoxia, depending on their origin. Particularly, hypobaric hypoxia is a type of hypoxia brought on by a reduction in total atmospheric pressure (Lopez-Ramos et al. 2005). Both hypoxia and reoxygenation (recovery of normal oxygen levels in blood

R. Hernández · S. Blanco (✉) · J. Á. Pedrosa · M. Á. Peinado
Area of Cellular Biology, Department of Experimental Biology (Building B-3), University of Jaén, Campus Las Lagunillas s/n, 23071 Jaén, Spain
e-mail: sblanco@ujaen.es

J. Peragón
Area of Biochemistry and Molecular Biology, Department of Experimental Biology, University of Jaén, Campus Las Lagunillas s/n, 23071 Jaén, Spain

and tissues) trigger different physiopathological signs, which may lead to transient or irreversible tissue alterations (Hodkinson 2011; LaManna et al. 2004; Rodrigo et al. 2005). The central nervous system is particularly vulnerable to hypoxia and especially to the oxidative stress generated after ischemia or hypoxia (Canuelo et al. 2007).

Currently, one of the most noteworthy areas, and perhaps the most challenging one, is the complex network of signals that are triggered after a hypoxic process; most of these signals are the consequence of changes in the expression and activity of certain proteins that deploy a cascade of events regulating the mechanisms of response to hypoxia (Taylor 2008). Today, we know that hypoxia can generate transcription factors such as the hypoxia-inducible factor 1 (HIF-1); in turn, HIF-1 stabilization stimulates the expression of certain genes and therefore of some critical proteins, which contribute to the generation of an adaptive response to hypoxia (Lopez-Barneo et al. 2001). Delving into these features, previous results of our model of hypobaric hypoxia (Canuelo et al. 2007; Martinez-Romero et al. 2012) have demonstrated that expression changes were induced in HIF-1 of the cerebral cortex (Martinez-Romero et al. 2009, 2012) as well as in the expression of some proteins involved in oxidative and nitrosative stress (Rodrigo et al. 2004). In addition, intensified protein nitration has been established immediately after the hypoxic insult in rat brains submitted to 30 min of hypobaric hypoxia (Castro-Blanco et al. 2003; Rodrigo et al. 2005).

Nevertheless, one of the first changes induced by hypoxia involves energetic metabolism; in fact, the consumption of scarce adenosine triphosphate (ATP) reserves within the cells, due to the limited oxygen supply, is among the most important events described after a hypoxic insult. These situations, apart from triggering the formation of free radicals, immediately stimulate greater ATP production. In short, hypoxia leads to a fall in ATP production but to a parallel ATP consumption, so that ultimately, the energy supply to the cells is interrupted (Harkness 1997). Thus, when the causes of hypoxia persist, the molecular mechanisms initially activated to avoid the energy collapse finally inflict irreparable damage that may even result in cell death (Cleveland 1996).

Besides free radical generation and energy depletion, another set of alterations affects neuronal-membrane protein integrity and fluidity, as well as cytoskeletal dysfunction, which also contribute to the neuronal death (Schwartz et al. 1993). In this respect, the role played by the cytoskeleton is crucial in promoting cell death, due to the misfolding of the proteins after hypoxia (Feldman et al. 2005), in which the helping protein chaperones also must play a key role (Giffard et al. 2004).

More recent studies have sought to ascertain the overall gene expression in hypoxic situations, as has been demonstrated specifically in chronic hypobaric hypoxia; in this model, inflammatory signaling networks occur as well as induction of an antioxidant defense system (Sethy et al. 2011). Consequently, it could be assumed that hypobaric hypoxia induces changes in some biomarkers, such as heat-shock protein 70 kDa (HSP70) or adrenomedullin, which are part of the hypoxic response (Julian et al. 2011), but at the moment, the molecular mechanisms underlying these alterations and the key factors that coordinately manage the final response just begin to arise (Maa 2010; Sethy et al. 2011).

Considering all this evidence, particularly the few studies and scant information concerning the changes on global protein expression in brain hypoxia, we propose a proteomic approach enabling the identification of the brain-cortex proteins that are differentially expressed in response to an acute hypobaric hypoxic episode and the subsequent reoxygenation in rat. This study will provide information about the way in which these proteins contribute to the response to hypoxia as well as new and relevant information about the molecular mechanisms that are triggered after the hypobaric hypoxia. To our knowledge, it is the first time that hypoxia-altered protein-expression pattern is described in the brain cortex.

Materials and Methods

Chemicals

Chemicals and materials used for 2-DE analysis were supplied by BioRad Laboratories (Hercules, USA) and GE Healthcare (Uppsala, Sweden). Specific reagents used for making buffers and other solutions came from Sigma–Aldrich Chemical Co. (St. Louis, USA) and Fluka (Buchs, Switzerland).

Animals

The study was performed on 20 adult male albino Wistar rats weighing 350 g each kept under standard conditions of light and temperature and allowed ad libitum access to food and water. All procedures were performed in accordance with the EU Directive 2010/63/EU (2010), reviewed by the Ethics Committee of the Spanish Council for Scientific Research, approved by the Committee of Bioethics of the University of Jaén, and are in accordance with the Uniform Requirements for manuscripts submitted to Biomedical Journals.

Hypobaric Hypoxia Model

Hypoxia was induced by downregulating the environmental O_2 pressure to an approximate final barometric pressure

of 316 hPa inside a hypobaric chamber. More specifically, hypobaric hypoxia was induced by using a slight modification of a previously published procedure (Lopez-Ramos et al. 2005; Martinez-Romero et al. 2006). Briefly, animals were introduced into a hypobaric chamber in which the air pressure was controlled by means of a continuous vacuum pump and an adjustable inflow valve. The chamber was also provided with a manometer to check the experimental altitude during the process. The conditions, simulating an altitude of 30,000 feet (8,810 m), were maintained for 1 h. Ascent and descent rates were kept below 1,000 feet/min. After the hypoxic period, the return to normobaric normoxic conditions (150 mmHg O_2 partial pressure in our setting) was attained in 30 min. Animals were either killed immediately after the hypobaric chamber was opened (0-h reoxygenation group) or kept at atmospheric pressure under standard conditions of light and temperature and allowed ad libitum access to food and water for 24 h or 5 days and then killed (24-h and 5-day reoxygenation group, respectively). Animals kept in the chamber under normobaric normoxic conditions served as controls.

Sample Preparation and Protein Extraction

After the corresponding reoxygenation times, the rats were killed by cervical dislocation, and the brain cortices of 5 rats of each group were dissected, rinsed in saline solution, frozen in liquid nitrogen, and stored at −80 °C until analyzed.

For extracting the proteins, 0.1 g of brain cortex was homogenized with 1.5 mL of extraction buffer pH 8, containing 8 M urea, 20 mM dithiothreitol (DTT), 100 mM HCl–Tris, 0.75 mM phenylmethylsulfonyl fluoride (PMSF), and 4 % 3-[(3-cholamidopropyl)-dimethylammonio]-1-propane sulfonate (CHAPS). For each experimental group, three replicates of the homogenates were made. Each replicate was made with a pool of the brain cortex of five rats. Proteins were extracted in this buffer for 60 min on ice. Every 15 min, the samples were moderately shaken in a vortex and afterward were centrifuged at 10,000×*g* for 15 min at 4 °C. The protein concentration of the supernatants was measured using the CB-XTM Protein Assay (G-Biosciences, St Louis, USA).

2-DE

Protein extracts (120 µg) were incubated 30 min in 450 µL rehydration buffer containing 8 M urea, 2 % CHAPS, 20 mM DTT, 0.5 % Pharmalyte 3–10, and bromophenol blue traces. The samples were loaded onto 18 cm (pH 3-11 NL) Immobiline Dry-Strips (GE Healthcare, Little Chalfont, UK). After 2 h of passive and 10 h of active (50 V) rehydration in a Protean IEF Cell (BioRad Laboratories, Hercules, USA) at 20 °C and 50 µA/strip, the voltage was raised to 1,000, 4,000, and 8,000 V in 120 min rapid, and to 8,000 V in 30 min linear. The sample was maintained at 8,000–50,000 V h, around 5 h. After isoelectric focusing, the strips were soaked 15 min in the equilibration buffer containing 50 mM Tris–HCl pH 8.8, 6 M urea, 30 % glycerol, 2 % sodium dodecyl sulfate (SDS), bromophenol blue traces, and 2 % DTT. After being drained, the strips were soaked again 15 min in this mix with 2.5 % iodoacetamide. SDS–PAGE was performed in 12 % gels using the Protean Plus Dodeca cell (BioRad Laboratories, Hercules, USA) at 8 °C and 30 V, 30 min, and 60 V until separation was finished. Gels were stained with Sypro Ruby® Protein Stain (BioRad Laboratories, Hercules, USA) compatible with MS analysis.

Quantitative Analysis of Gel Images and Statistical Analysis

Once gels were digitalized (GS-800 densitometer, BioRad Laboratories, Hercules, USA), in order to facilitate single-spot identification, the image background was subtracted by means of ImageJ 1.44 application (National Institute of Mental Health, Bethesda, USA) using the same value for each image. Adobe Photoshop PS (Adobe Systems Incorporated, San Jose, USA) was used for the comparative study of images. Hence, paired images of any two groups compared were opened simultaneously and then overlaid. Shadow-color equilibrium of the upper layer was adjusted until reaching the desired color dominance of the spots. Finally, the opacity of the upper layer was cleared in order to achieve an easy scroll over the lower layer, to facilitate the comparison between upper and lower spots. Only spots exhibiting an over/underexpression ratio of at least twofold with respect to any other sampling site were considered. One-way analysis of variance (ANOVA) followed by Student's *t* test was then used for a definitive selection of the spots showing altered expression patterns between any two groups.

Protein Digestion and MS Analysis

Differentially expressed spots were automatically excised in an Investigator ProPic station (Genomic Solutions, Huntingdon, UK). The gel pieces were digested with trypsin using a Progest station (Genomic Solutions, Huntingdon, UK) under the following conditions: two steps of unstaining for 30 min with 50 % acetonitrile (ACN)/100 mM ammonium bicarbonate; a step of dehydration with 100 % ACN for 5 min and dryness of the sample; two steps of washing with 25 mM ammonium bicarbonate for 15 min; two steps of washing with 25 mM ammonium bicarbonate/50 % ACN for 15 min; a step of dehydration

with 100 % ACN for 5 min and dryness of the sample; a step of hydration with 10 μL of 12.5 ng μL-1 trypsin in 25 mM ammonium bicarbonate for 10 min at room temperature; and finally, digestion in a microwave for 2 steps of 5 min each. The digestion was stopped by adding 1 μL of 10 % trifluoroacetic acid (TFA). The peptides obtained were purified in a ProPrepII (Digilab, Holliston, USA) with a C18 microcolumn (ZipTip, Millipore, Billerica, USA), eluting with a matrix solution (3 mg mL-1 α-cyano-4-hydroxycinnamic acid dissolved in 70 % ACN/0.1 % TFA). Eluted samples were directly spotted onto a MALDI plate at a volume of 1 μL.

Samples were analyzed by MALDI-TOF/TOF in a 4800 Proteomics Analyzer Spectrometer (Applied Biosystems, Foster City, USA). The instrument operated in the positive reflection delayed extraction mode. Spectra were internally calibrated using the m/z ratios of the peptides found by the autodigestion of porcine trypsin ($M^+H^+ = 842.509$, $M^+H^+ = 2{,}211.104$). The m/z was measured to a precision of ±20 ppm. The MS/MS fragmentation spectra of the most intense 12 m/z fragments were found for each sample. The spectra found in the MALDI-TOF/TOF analysis were adjusted to a base line, the signal/noise threshold peak was 10, and the peaks were de-isotoped. Finally, the values of the mono-isotope ions of each peptide were detected.

Database Searching

Molecular masses of the tryptic peptide profiles produced were used to search the National Center for Biotechnology Information (NCBI) nucleotide non-restricted database using the MASCOT program (Matrix Science, London, UK). The peptide masses were compared to the theoretical peptide masses of all available proteins and predicted proteins from DNA sequences. All peptide fragments obtained for each digest were submitted to a search, which was made by combining PMF and the results from MS/MS fragmentations. The search parameters were as follows: maximum allowed error of peptide mass 100 ppm, considered modifications, methionine oxidation, carbamidomethyl cysteine, the formation of pyroglutamic acid, and the possible acetylation of N-terminal extreme.

Western Blot Analysis

For Western blot analysis, samples from the same animals assessed for the proteomic study were used. Tissues were homogenized in 1/3 (w/v) of 30 mM Tris–HCl, pH 7.4, containing 0.5 mM DTT, 1 mM EDTA, 1 % SDS, and protease inhibitors cocktail (Roche, Basel, Switzerland). The resulting homogenates were centrifuged for 1 h at 100,000×*g*. All the procedures were performed at 4 °C. The protein concentrations in the supernatants were determined by the Bradford method (Bradford 1976). Equal amounts (20 μg) of the denatured proteins per lane were loaded and separated on NuPAGE® Novex 4–12 % Bis–Tris Gels (Invitrogen, Carlsbad, USA) as described by Laemmli (1970). Afterward, proteins were transferred to a PVDF membrane using the XCell SureLock™ Mini-Cell system (Invitrogen, Carlsbad, USA). The membranes were blocked with 2.5 % powdered nonfat milk in 25 mM Tris–HCl, pH 7.6, 137 mM NaCl, 2.6 mM KCl, and 0.1 % Tween 20 and incubated overnight at 4 °C with diluted goat polyclonal anti-γ-enolase (1:500, Santa Cruz Biotechnology, INC, Santa Cruz, USA); rabbit polyclonal anti-heat-shock protein 72 kDa (1:1,000, Enzo® Life Sciences, USA); mouse monoclonal anti-α-tubulin (1:14,000, Sigma, St. Louis, USA); mouse monoclonal anti-β-actin (1:5,000, Sigma, St. Louis, USA); and rabbit polyclonal anti-glyceraldehyde 3-phosphate dehydrogenase (1:20,000, Santa Cruz Biotechnology, INC, Santa Cruz, USA), in blocking solution. Bound antibody was revealed by means of an enhanced chemiluminescence kit (Amersham ECL Prime Western blotting detection reagent, GE Healthcare, Little Chalfont, UK) according to the manufacturer's instructions. The amount of the proteins in each sample was quantified by densitometric scanning and expressed as arbitrary units (AU).

Statistical Treatment

Data were expressed as mean ± SD. Statistical comparisons between reoxygenation groups and the corresponding control group were made by ANOVA followed by Student's *t* test, accepting $p < 0.05$ as the level of significance.

Results

Generation of the 2-DE Reference Pattern for Rat Brain-Cortex Proteins

Protein extracts from the brain cortex of control and hypoxic/reoxygenated rats were analyzed by 2-DE. For each group, three gels were made (12 gels in total). Figure 1 shows the master gel with the superposition of all spots detected in these 12 gels. This master gel was chosen as a reference gel for the study, and the profiles of other gels were matched against it. The isoelectric point (p*I*) ranged from 4.79 to 8.43.

Detection of Differentially Expressed Proteins

The criteria followed in order to detect changes in protein expression in all the experimental groups were as follows: (1) a 2-fold difference in spot abundance between the control and experimental groups and (2) a consistency in the change for the three replicate analyses per group. Thus, the

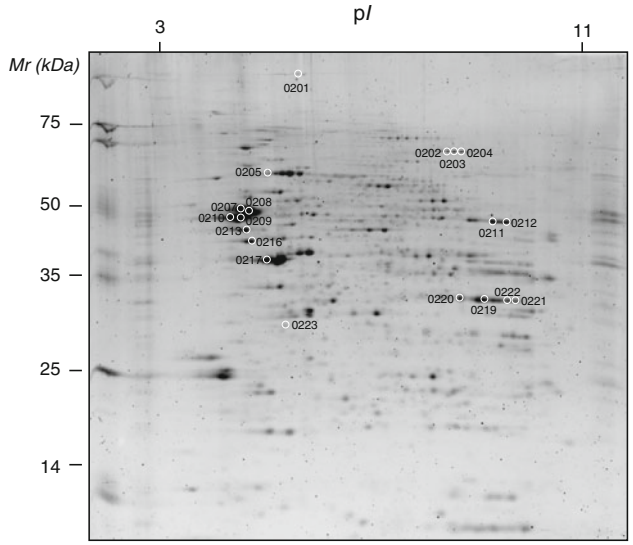

Fig. 1 2-DE gel of cerebral-cortex proteins of rats under hypoxia and reoxygenation conditions. Proteins (120 μg) were separated in the first dimension on pH 3-11 IPG strips, followed by SDS–PAGE on 12 % w/v gels. Gels were stained with Sypro Ruby®. The spots excised for MALDI-TOF/TOF analysis are *encircled*

quantitative analysis of the gels yielded 19 spots (Table 1) with significantly altered expression. The locations of such spots are indicated in Fig. 1. These spots were excised from the gels and digested with trypsin, and the resulting peptide fragments were analyzed by MS and MS/MS.

Identification of Protein Spots

The results found with the MS and MS/MS analyses were used to make a combined database search. The results of the identification are shown in Table 1. Identifications relied on three matched peptides. Searches were made against all organism databases using major spectral peaks and matching errors 50 ppm. Most listed matches gave good MOWSE scores and high sequence coverage. Nineteen spots were identified from protein or cDNA sequences already described in the following species: *Rattus norvegicus*, *Mus musculus*, *Macaca mulatta*, and *Homo sapiens*. The spots identified corresponded to 11 different proteins. In five cases (aconitate hydratase, α-tubulin, β-tubulin, F1-ATPase chain α, and GAPDH), various spots were identified with a different variant of the same protein. In all cases, the variants detected were located in the horizontal direction of the gel. These variants can be explained by charge changes caused by posttranslational modifications that explained the differences reported.

Grouping Spots by Putative Functionality

The proteins identified were grouped into several categories according to their similarity in function or to their involvement in the same metabolic pathway. Thus, we distinguished five groups: (1) glycolysis proteins, including NSE and GAPDH; (2) tricarboxylic acid cycle proteins, such as aconitate hydratase (ACO2); (3) oxidative phosphorylation proteins, such as F1-ATPase chains α and β; (4) cytoskeleton proteins, including the non-erythroid α-spectrin 2 (Spna2), α-tubulin, β-tubulin, β-actin, and microtubule-associated protein RP/EB family member 3 (MAPR3 or EB3); and (5) chaperones, such as heat-shock protein 72 kDa (HSP72) (Fig. 2).

Data Validation by Western Blot Analysis

To validate the results of the proteome analysis, we performed the Western blot for one protein (NSE) upregulated after hypobaric hypoxia, and four downregulated proteins (α-tubulin, β-actin, GAPDH, and HSP72). The expression patterns for these analyses (Fig. 3) are similar to those detected by the 2D proteomic approach for the five proteins assayed.

The main proteins that are routinely used as loading control markers were observed to be altered in this study. Thus, we determined to show the total protein data of the samples, instead of a loading control, in order to clarify that the differences found in the Western blot of the proteins analyzed are really due to expression changes and not to variations in total protein content among any experimental group or controls. The data are shown in Fig. 3 caption.

Discussion

Exposure to hypoxia reportedly provokes neurological disorders such as memory deficits as well as coordination and motor impairment (Bahrke and Shukitt-Hale 1993; Hamilton et al. 1991). However, regardless of the importance of these diseases, the data on the molecular mechanisms that take place after an in vivo model of brain hypobaric hypoxia are still scarce. In this sense, this study has used the proteomic analysis, as the appropriate methodology, to identify the main proteins that undergo changes after this insult in order to provide the basis for further molecular mechanisms after an episode of hypobaric hypoxia. Hence, our results suggest that an acute hypobaric hypoxic insult triggers in the brain cortex a number of changes in the expression of many proteins involved in different key pathways associated with energy metabolism, particularly glycolysis, tricarboxylic acid cycle, and oxidative phosphorylation, as well as with cytoskeleton and protein folding.

Energetic Metabolism

We detected expression changes for NSE and GADPH, both involved in the glycolysis; for ACO2, a mitochondrial

Table 1 Results from peptide mass fingerprinting of protein spots excised from 2-DE gels

Spot[a]	Identification	Species	Mass (kDa)	pI	Peptides matches[b]	Accession number (gi)	Mowse Score[c]	% Coverage[d]
0201	Spna2[e]	*Rattus norvegicus*	283.00	5.19	44	47477769	392	22
0202	ACO2[f]	*Rattus norvegicus*	86.12	7.87	26	40538860	763	40
0203	ACO2	*Rattus norvegicus*	86.12	7.87	27	40538860	730	42
0204	ACO2	*Rattus norvegicus*	86.12	7.87	24	40538860	528	38
0205	HSP72 [g]	*Rattus norvegicus*	71.11	5.43	22	347019	721	48
0207	α-Tubulin	*Macaca mulatta*	48.22	4.97	18	109096482	782	57
0208	α-Tubulin	*Macaca mulatta*	45.31	4.94	18	109096498	941	62
0209	β-Tubulin	*Rattus norvegicus*	50.22	4.79	20	40018568	703	48
0210	β-Tubulin	*Homo sapiens*	50.28	4.82	20	27227551	654	48
0211	F1-ATPase, chain α	*Rattus norvegicus*	55.34	8.28	27	93279422	708	60
0212	F1-ATPase, chain α	*Rattus norvegicus*	55.36	8.28	23	6729934	1,100	54
0213	F1-ATPase, chain β	*Rattus norvegicus*	51.32	4.95	19	6729935	1,050	53
0216	NSE[h]	*Rattus norvegicus*	47.51	5.03	18	26023949	528	55
0217	β-actin	*Mus musculus*	39.44	5.78	15	49868	661	61
0219	GAPDH[i]	*Rattus norvegicus*	36.09	8.14	14	8393418	686	48
0220	GAPDH	*Rattus norvegicus*	36.09	8.43	14	56188	519	54
0221	GAPDH	*Rattus norvegicus*	36.09	8.43	15	56188	708	49
0222	GAPDH	*Rattus norvegicus*	36.09	8.14	15	8393418	592	54
0223	EB3[j]	*Mus musculus*	36.34	5.57	6	148705348	72	22

[a] The ID number refers to spots listed in Fig. 1

[b] Number of peptides fragmented with homology

[c] MASCOT score > score corresponding to $p < 0.001$ (probability > 99.9 %)

[d] Coverage percentage of the peptide sequence homology

[e] *Spna2* non-erythroid α-spectrin 2

[f] *ACO2* aconitate hydratase

[g] *HSP72* heat-shock protein 72 kDa

h NSE γ-enolase

[i] *GAPDH* glyceraldehyde 3-phosphate dehydrogenase

[j] *EB3* microtubule-associated protein RP/EB family member 3

key enzyme involved in the tricarboxylic acid cycle, and for F1-ATPase, the main enzyme responsible for ATP production in the respiratory mitochondrial chain.

NSE is a neuron-specific enolase that regulates an important step of glucose metabolism; specifically, it catalyzes the conversion of 2-phospho-D-glycerate into phosphoenolpyruvate and water, although it also exhibits a number of regulatory properties in the brain (Pancholi 2001). It is located in neuronal bodies, axons, and neuroendocrine cells (Moore and McGregor 1965; Schmechel et al. 1978). After neuronal or blood–brain barrier damages, it can leak into extracellular compartment and the bloodstream (Guzel et al. 2008); this makes NSE an excellent serum biomarker of neuronal injury (Bailey et al. 2011), including hypoxic/ischemic encephalopathy damage (Celtik et al. 2004). NSE has been described as a target of HIF-1, one of the main genes involved in the hypoxic response (Griffiths et al. 2007; Pacary et al. 2007). Our model of hypobaric hypoxia induces a progressive and significant increase in NSE expression during hypoxia/reoxygenation, which peaks after 5 days of reoxygenation. This rise suggests an upregulation of the glycolytic neuron metabolism, probably as a belated attempt (higher levels of NSE are found after 5 days of reoxygenation) to restore the depleted energy and to avoid the oxygen-deprivation-related damage that alters the main metabolic pathways within the cerebral cortex.

Besides the classical role of GAPDH in the catalysis of glyceraldehyde 3-phosphate to D-glycerate 1,3-bisphosphate, it has also been implicated in other non-metabolic processes that may influence neurodegeneration; these include roles in membrane fusion and endocytosis, microtubule binding, nuclear translocation in apoptosis, and interaction with the nitric oxide pathway (Sirover 2011). It is known that GAPDH expression is regulated by hypoxia (Graven et al. 1998) and that hypoxia leads to the

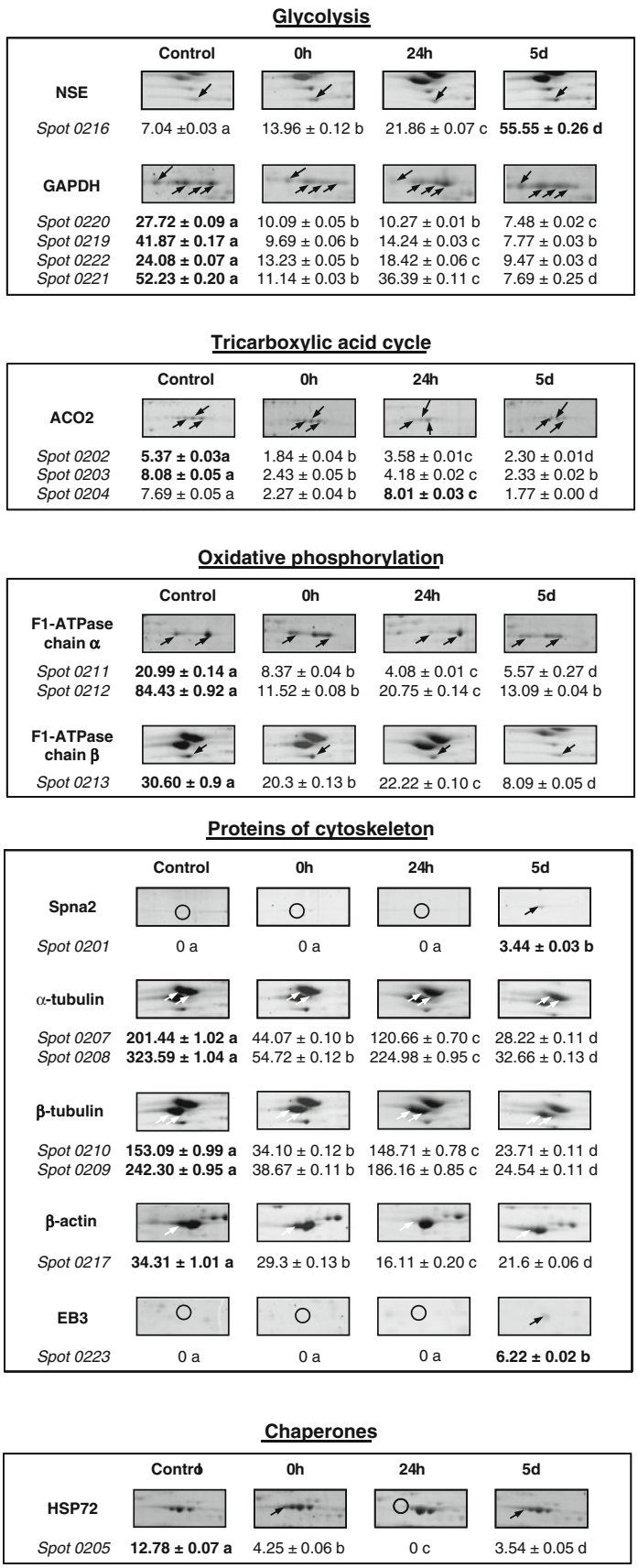

Fig. 2 Focal 2-DE gel images showing differential expression of the eleven identified proteins that changed in response to hypoxia and reoxygenation (0 h, 24 h, and 5 d). Proteins are grouped according to their function into five categories: (1) glycolysis proteins, (2) tricarboxylic acid cycle proteins, (3) oxidative phosphorylation proteins, (4) cytoskeleton proteins, and (5) chaperones. The abbreviations used for the proteins are explained in Table 1. The *arrows* indicate the intense spots and the *circles* the faint or practically absent spots. *Numbers in boldface* indicate the sites with the highest volumes. Spot volumes (in arbitrary units) are given as mean ± SEM below representative 2-DE gel sections. Values followed by *different letters* are significantly different ($p < 0.05$)

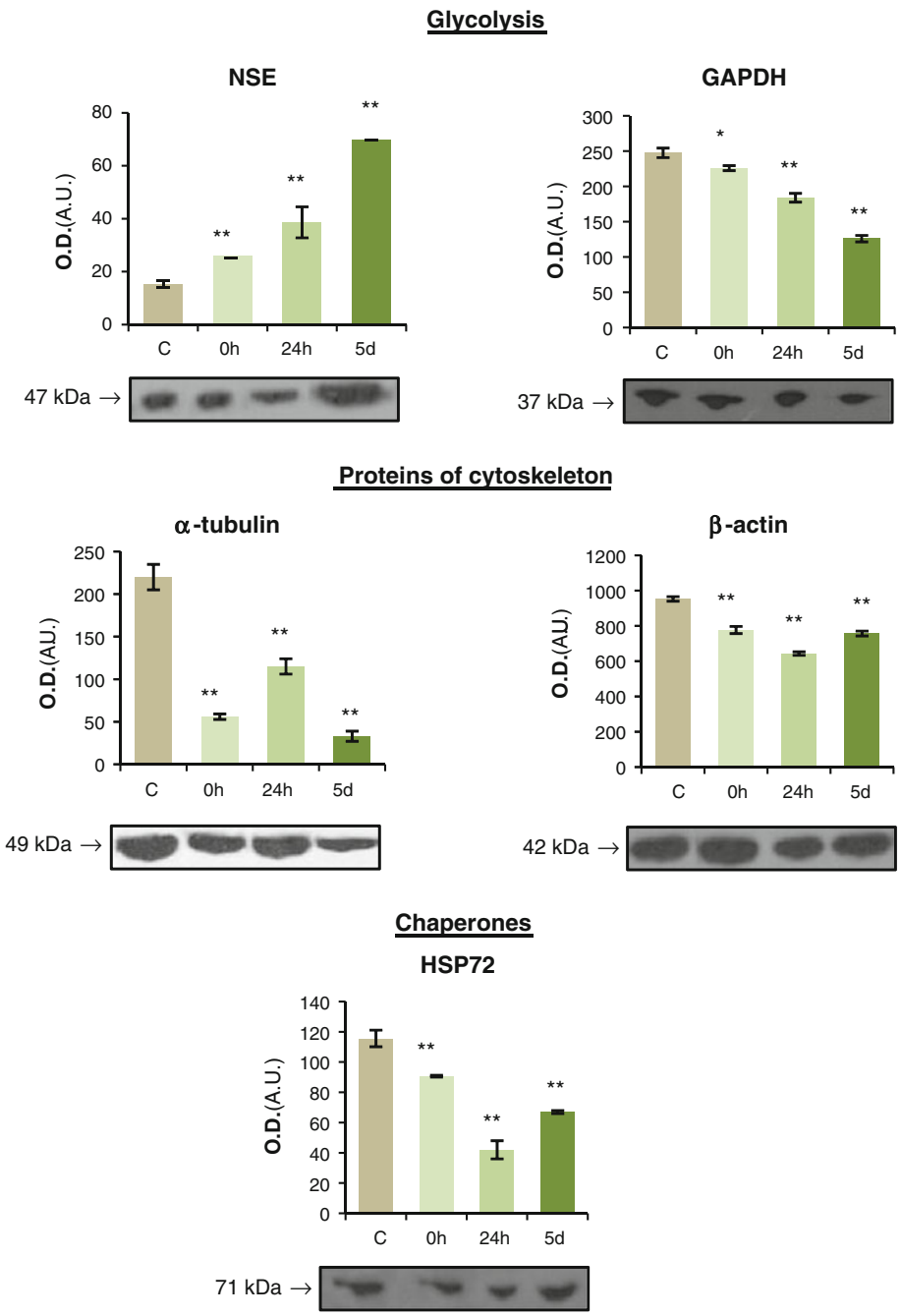

Fig. 3 Western blot analysis of NSE, GAPDH, α-tubulin, *β*-actin, and HSP72 in brain-cortex cytosolic extracts of control (control) and experimental (0 h, 24 h, and 5 days) rats. The expression patterns found are similar to those detected by the 2D proteomic approach (Fig. 2). Proteins were separated by Novex 4–12 % Bis–Tris gels and then blotted onto a PVDF membrane. The amount of protein load per lane was 20 µg. The polypeptide corresponding to the monomeric form of the proteins was detected with specific antiserum. The quantification of protein levels by densitometric analysis is shown in *bar graphics*. The results are average values of five experimental animals in each group. Data are the mean ± SEM of five values and are expressed as arbitrary units of integrated optical density. *Bars with asterisks* are significantly different ($p < 0.05$). *OD* optical density, *AU* arbitrary units. Total protein amount of samples showed no significant differences between any experimental group and control. Data (mean ± SEM) are expressed in mg/ml: *C*, 4.61 ± 0.24; 0 h, 4.56 ± 0.27; 24 h, 5.00 ± 0.19; 5 days, 5.09 ± 0.29

formation of a complex in the cytoplasm through the aggregation of GAPDH with the TOAD64 protein, NSE, aldolase C, and HSP70; this complex appears to play a role in membrane fusion and intracellular signaling (Bulliard et al. 1997; Nakamura et al. 2002). GAPDH also acts as an NO sensor, showing functional alterations when nitrosylated, as reported in situations of toxic NO supply such as Alzheimer's disease (Hara et al. 2006; Sultana et al. 2006). Nevertheless, it has been observed that S-glutathionylation serves as a temporary shield (Batthyany et al. 2006), allowing GAPDH to continue to function once the redox state of the cell returns to normality. In this sense, it has been observed that the decreased oxidation of GAPDH could lead to improved glycolytic function and increased ATP production leading to a possible neuronal recovery and improved cognitive function as has been reported in a canine model of aging (Opii et al. 2008). After hypoxia, our results showed that, contrary to NSE, GAPDH undergoes a progressive decrease during the reoxygenation periods, which reaches the lowest level at 5 days post-hypoxia. The sensitivity of GAPDH to oxidation might explain our results, as the decrease in GAPDH expression

detected could be the result of the overoxidation of GAPDH during the reestablishment of the oxygen supply (reoxygenation), which in turn could lead to an impairment of its function and even to a possible degradation.

ACO2 is a mitochondrial enzyme that catalyzes the isomerization of citrate to isocitrate via cis-aconitate in the tricarboxylic acid cycle. ACO2 has been found to be specifically targeted by oxidative damage during aging (Addabbo et al. 2009; Hendgen-Cotta et al. 2008), and its activity has been shown to be sensitive to superoxide and peroxynitrite ($ONOO^-$) damage through oxidation of the iron–sulfur centers (Gardner et al. 1994). In our experimental model, ACO2 expression decreased significantly in all the reoxygenation periods, and as with GAPDH, its sensitivity to oxidative-derived damage could be responsible for such decline.

F1-ATPase is one of the most abundant proteins in all organisms. It is responsible for synthesizing the molecule ATP, coupled to the mitochondrial electron transport chain. This fact reveals the close relationship between this molecule and the hypoxic phenomena. In this sense, 30 days of hypoxic exposure affects the expression of mitochondrial F1-ATPase chain α in rat skeletal muscle, weakening the stability of the mitochondrial membrane and mitochondrial electron transport chain (Chen et al. 2012). Our results reflect lower F1-ATPase expression with hypoxia in both the α and β chains; these results could be due to the loss of proteins coupled with the destabilization of the mitochondria found after a hypobaric hypoxic insult (Nouette-Gaulain et al. 2011), which would alter both the structure and functionality of ATPase, and more specifically its catalytic subunit F1.

Proteins of Cytoskeleton

We have found changes in the expression of both cytosolic (EB3, α-tubulin, β-tubulin, and β-actin) and membrane-associated (Spna2) cytoskeletal proteins, responsible for maintenance of cellular structure and function.

Spectrin is a membrane cytoskeletal protein that consists of α and β subunits. More specifically, the α-fodrin or non-erythroid α-spectrin 2 (Spna2) possesses high affinity for calmodulin and calcium-binding site. Spna2 maintains the membrane integrity (Voas et al. 2007) and interacts with integral membrane protein, such as ion channels (Bennett and Lambert 1991). Spectrin breakdown product by calpain has been detected in different brain pathologies including focal ischemia in rats (Hong et al. 1994; Pike et al. 2004). Thus, this protein has been proposed as an early marker in a variety of central nervous system injuries including ischemia (Aikman et al. 2006; Dutta et al. 2002). Our results indicate that Spna2 is not expressed either in control or immediately after the hypoxic hypobaric episode; however, after 5 days of reoxygenation, a new expression of this protein takes place in the injured brain cortex. These results are consistent with those from other authors (Chen et al. 2007; Indraswari et al. 2009), who found that this protein was upregulated after medial cerebral artery occlusion in rat. However, as opposed to Chen et al. (2007), we found only one spot identified as Spna2, within the range of the theoretical value of 280 kD (Winkelmann and Forget 1993), but not Spna2 breakdown products, as they also reported (Chen et al. 2007). These data might suggest that our model of sole hypobaric hypoxia does not cause fragmentation of Spna2 found in other models that imply a more aggressive hypoxic insult.

Microtubule-associated protein RP/EB family member 3 (MAPR3 or EB3) is a protein localized in the cytoplasmic microtubule network. It is expressed predominantly in brain (Akhmanova et al. 2005; Komarova et al. 2005; Lansbergen and Akhmanova 2006) and is involved in regulating cellular adhesion. In this sense, EB3 participates in microtubule polymerization and spindle function by stabilizing microtubules and anchoring them at centrosomes and may play a role in cell migration (Sweet et al. 2011). Our data show that EB3 expression, like Spna2, appears only after 5 days of reoxygenation, although its potential role after hypoxia will require further investigation.

The most common members of the tubulin family, α- and β-tubulin, are synthesized and actively transported down the axon to assemble microtubules that regulate neuronal polarization, axon growth, remodeling of dendritic spines, and transport of cargo molecules (Baas 1997; Janke and Kneussel 2010).

Both α- and β-tubulins show a parallel expression pattern in our experimental model—that is, at 0 h, the levels significantly fell, but strongly recovered after 24 h of reoxygenation. Accordingly, previous studies have also demonstrated that the content of α-tubulin is changed early in the post-hypoxic period in neurons (Raley-Susman and Murata 1995). Thus, our results would support the conception that the neuronal cytoskeletal protein has high sensitivity and probably vulnerability to hypoxia, a situation that would be consistent with the results found in an experimental rat model of intermittent in vivo hypoxia (Shen and Yu 2008). However, our data also show a significant fall, even to lower levels than control, of tubulin expression at extended reoxygenation times (5 days). These changes during the reoxygenation periods may suggest that a new reorganization of the cytoskeleton is triggered at a later time after the hypoxic insult. In this connection, hypoxia also raised the growth-cone level of α-tubulin but did not increase its mRNA expression, which may indicate an inability to polymerize tubulin and to build microtubules at later reoxygenation times. (Morgan and

Chao 2004). A deeper examination of this fact has revealed that an insufficient neurofilament synthesis with anomalous components of neurofilament subunits, β-tubulin, and MAP2 isoforms indicates immaturity of axons in intermittent hypoxia-exposed brains in mice between postnatal days 2 and 10 (Cai et al. 2012).

Actin is one of the major components of the cytoskeleton, so it participates in many important cellular processes, including vesicle and organelle movement, cell motility, cytokinesis, the establishment and maintenance of cell junctions and cell shape, as well as cell signaling. Most of these main cellular processes are mediated by close interactions of actin with cell membranes, inducing changes that affect synaptic transmission and plasticity (Bosch and Hayashi 2012). Three main groups of actin isoforms are known in vertebrates; specifically, β-actin appears in most cell types as a component of the cytoskeleton. Furthermore, actin exists in an ATP-dependent dynamic equilibrium between its monomeric and filamentous states (Friedman et al. 1998). Our data show that, like tubulins, β-actin expression is downregulated after all the reoxygenation periods compared to control. In this sense, other authors have reported that lowering O_2, and probably in part through HIF-1, alters the expression of tubulin and β-actin (Ostergaard et al. 2009). Our results may suggest the notion that the cytoskeleton of brain-cortex cells is highly sensitive to hypobaric hypoxia and indicates that this situation may induce a cytoskeleton restructuring, possibly to maintain cellular functionality. Accordingly, a proteomic study carried out in cell culture submitted to two forms of hypoxia (1 % O_2 and 5 % O_2) suggests as well that the hypoxia-derived cytoskeletal changes may be due partly to the decrease in β-actin (Ostergaard et al. 2009).

Chaperones

HSP72 is a stress-inducible form of cytosolic HSP70 which has strong cytoprotective effects and which functions as a molecular chaperone in protein folding, transport, and degradation (Gupta et al. 2010). This protein operates in an ATP-dependent manner and is expressed at low levels under physiological conditions, but it is induced upon exposure to situations that may cause cytosol protein misfolding, such as heat shock, anoxia, and ischemia (Morimoto et al. 1997; Tavaria et al. 1996). In a model of heart ischemia, it was reported that the expression of HSP72 appears to be via the adenosine A1 receptor and ATP-sensitive potassium channel although it does not involve the synthesis of HSP72 (Bernardo et al. 1999). On the contrary, in neurons, although a protective mechanism against ischemia–reperfusion insult was also associated with enhanced expression of HSPs, the induction mechanism seems to be independent of the opening of the potassium channels (Reshef et al. 2000). On the other hand, in a model of middle cerebral artery occlusion, it was found that overexpression of HSP70 significantly improves neurological scores and shows smaller infarcts than in control animals (Zhao et al. 2006). In addition, it has also been found that HSP72 overexpression preserves mitochondrial-membrane potential in an in vitro model of oxygen and glucose deprivation (Ouyang et al. 2006). Moreover, after sublethal ischemic preconditioning, the expression of HSP70 mRNA is accelerated after a second longer ischemia; under these conditions, the levels of HSP70 mRNA peaked at 3 h after the ischemia and then gradually declined to disappear at 24 h post-hypoxia (Heurteaux et al. 1995). In our experimental model of hypobaric hypoxia, HSP72 expression decreased after hypoxia (0 h), reaching the lowest level at the 24-h reoxygenation point and increasing slightly after 5 days of reoxygenation. Although, as stated above, HSP72 can be induced in certain critical situations, lower HSP72 levels can also be linked to enhanced susceptibility of neurons to pathological conditions including ischemia or excitotoxicity (Planas et al. 1997). This fact is consistent with our results, where not only a decrease in HSP72 expression, but a downregulation of the energetic metabolism after hypobaric hypoxia is observed as well; so, this energetic depletion would increase neuron vulnerability and in turn decrease HSP72 induction. Finally, as a consequence of all these events, lower HSP72 levels would affect the repair and subsequent remodeling of the cytoskeleton also detected by us, as described above.

Conclusions

In summary, the brain-cortex proteomic profile undergoes a number of changes after an in vivo model of hypobaric hypoxia/reoxygenation that affect proteins involved in crucial molecular pathways essential for the correct neuronal function. Hence, taking into account all the above, it could be stated that a close relationship exists between energy metabolism, the cytoskeleton, and chaperones in the complex molecular network that underlies the process of response to hypoxia. These findings could be the basis for the molecular mechanisms that trigger hypobaric hypoxia and that may mean the starting point for future works to pursue the search for therapeutic targets against hypoxia-related damage.

Acknowledgments This work was supported by the Spanish Ministry of Science and Innovation (SAF2008-03938). The proteomic analysis was carried out in the Proteomic Unit of the Research Technical Services of the University of Córdoba (Spain), a member of ProteoRed (The Spanish Proteomics Network). We thank Carlos A. Fuentes and Raquel Gonzalez for technical expertise during the

proteomics studies. We wish to thank Mr. David Nesbitt for his editorial help with the English version of the manuscript.

Conflict of interest The authors declare that they have no conflict of interest.

References

Addabbo, F., Ratliff, B., Park, H. C., Kuo, M. C., Ungvari, Z., Csiszar, A., et al. (2009). The Krebs cycle and mitochondrial mass are early victims of endothelial dysfunction: Proteomic approach. *American Journal of Pathology, 174*(1), 34–43.

Aikman, J., O'Steen, B., Silver, X., Torres, R., Boslaugh, S., Blackband, S., et al. (2006). Alpha-II-spectrin after controlled cortical impact in the immature rat brain. *Developmental Neuroscience, 28*(4–5), 457–465.

Akhmanova, A., Mausset-Bonnefont, A. L., van Cappellen, W., Keijzer, N., Hoogenraad, C. C., Stepanova, T., et al. (2005). The microtubule plus-end-tracking protein CLIP-170 associates with the spermatid manchette and is essential for spermatogenesis. *Genes & Development, 19*(20), 2501–2515.

Baas, P. W. (1997). Microtubules and axonal growth. *Current Opinion in Cell Biology, 9*(1), 29–36.

Bahrke, M. S., & Shukitt-Hale, B. (1993). Effects of altitude on mood, behaviour and cognitive functioning. A review. *Sports Medicine, 16*(2), 97–125.

Bailey, D. M., Taudorf, S., Berg, R. M., Lundby, C., Pedersen, B. K., Rasmussen, P., et al. (2011). Cerebral formation of free radicals during hypoxia does not cause structural damage and is associated with a reduction in mitochondrial PO2; evidence of O2-sensing in humans? *Journal of Cerebral Blood Flow and Metabolism, 31*(4), 1020–1026.

Batthyany, C., Schopfer, F. J., Baker, P. R., Duran, R., Baker, L. M., Huang, Y., et al. (2006). Reversible post-translational modification of proteins by nitrated fatty acids in vivo. *Journal of Biological Chemistry, 281*(29), 20450–20463.

Bennett, V., & Lambert, S. (1991). The spectrin skeleton: From red cells to brain. *Journal of Clinical Investigation, 87*(5), 1483–1489.

Bernardo, N. L., Okubo, S., Maaieh, M. M., Wood, M. A., & Kukreja, R. C. (1999). Delayed preconditioning with adenosine is mediated by opening of ATP-sensitive K(+) channels in rabbit heart. *American Journal of Physiology, 277*(1 Pt 2), H128–H135.

Bosch, M., & Hayashi, Y. (2012). Structural plasticity of dendritic spines. *Current Opinion in Neurobiology, 22*(3), 383–388.

Bradford, M. M. (1976). A rapid and sensitive method for the quantitation of microgram quantities of protein utilizing the principle of protein–dye binding. *Analytical Biochemistry, 72*, 248–254.

Bulliard, C., Zurbriggen, R., Tornare, J., Faty, M., Dastoor, Z., & Dreyer, J. L. (1997). Purification of a dichlorophenol–indophenol oxidoreductase from rat and bovine synaptic membranes: Tight complex association of a glyceraldehyde-3-phosphate dehydrogenase isoform, TOAD64, enolase-gamma and aldolase C. *Biochemical Journal, 324*(Pt 2), 555–563.

Cai, J., Tuong, C. M., Zhang, Y., Shields, C. B., Guo, G., Fu, H., et al. (2012). Mouse intermittent hypoxia mimicking apnoea of prematurity: Effects on myelinogenesis and axonal maturation. *Journal of Pathology, 226*(3), 495–508.

Canuelo, A., Siles, E., Martinez-Romero, R., Peinado, M. A., & Martinez-Lara, E. (2007). The nitric oxide system response to hypoxia/reoxygenation in the aged cerebral cortex. *Experimental Gerontology, 42*(12), 1137–1145.

Castro-Blanco, S., Encinas, J. M., Serrano, J., Alonso, D., Gomez, M. B., Sanchez, J., et al. (2003). Expression of nitrergic system and protein nitration in adult rat brains submitted to acute hypobaric hypoxia. *Nitric Oxide, 8*(3), 182–201.

Celtik, C., Acunas, B., Oner, N., & Pala, O. (2004). Neuron-specific enolase as a marker of the severity and outcome of hypoxic ischemic encephalopathy. *Brain Development, 26*(6), 398–402.

Chen, J., Gao, Y., Liao, W., Huang, J., & Gao, W. (2012). Hypoxia affects mitochondrial protein expression in rat skeletal muscle. *OMICS: A Journal of Integrative Biology, 16*(3), 98–104.

Chen, A., Liao, W. P., Lu, Q., Wong, W. S., & Wong, P. T. (2007). Upregulation of dihydropyrimidinase-related protein 2, spectrin alpha II chain, heat shock cognate protein 70 pseudogene 1 and tropomodulin 2 after focal cerebral ischemia in rats—a proteomics approach. *Neurochemistry International, 50*(7–8), 1078–1086.

Cleveland, D. W. (1996). Neuronal growth and death: Order and disorder in the axoplasm. *Cell, 84*(5), 663–666.

Dutta, S., Chiu, Y. C., Probert, A. W., & Wang, K. K. (2002). Selective release of calpain produced alphaII-spectrin (alpha-fodrin) breakdown products by acute neuronal cell death. *Biological Chemistry, 383*(5), 785–791.

EU Directive 2010/63/EU. (2010). Directive 2010/63/EU of the European Parliament and of the Council of 22 September 2010 on the protection of animals used for scientific purposes (text with EEA relevance). *Official Journal of the European Union, L276*, 33–79.

Feldman, D. E., Chauhan, V., & Koong, A. C. (2005). The unfolded protein response: A novel component of the hypoxic stress response in tumors. *Molecular Cancer Research, 3*(11), 597–605.

Friedman, J. E., Chow, E. J., & Haddad, G. G. (1998). State of actin filaments is changed by anoxia in cultured rat neocortical neurons. *Neuroscience, 82*(2), 421–427.

Gardner, P. R., Nguyen, D. D., & White, C. W. (1994). Aconitase is a sensitive and critical target of oxygen poisoning in cultured mammalian cells and in rat lungs. *Proceedings of National Academy of Science USA, 91*(25), 12248–12252.

Giffard, R. G., Xu, L., Zhao, H., Carrico, W., Ouyang, Y., Qiao, Y., et al. (2004). Chaperones, protein aggregation, and brain protection from hypoxic/ischemic injury. *Journal of Experimental Biology, 207*(Pt 18), 3213–3220.

Graven, K. K., McDonald, R. J., & Farber, H. W. (1998). Hypoxic regulation of endothelial glyceraldehyde-3-phosphate dehydrogenase. *American Journal of Physiology, 274*(2 Pt 1), C347–C355.

Griffiths, E. A., Pritchard, S. A., McGrath, S. M., Valentine, H. R., Price, P. M., Welch, I. M., et al. (2007). Increasing expression of hypoxia-inducible proteins in the Barrett's metaplasia–dysplasia–adenocarcinoma sequence. *British Journal of Cancer, 96*(9), 1377–1383.

Gupta, S., Deepti, A., Deegan, S., Lisbona, F., Hetz, C., & Samali, A. (2010). HSP72 protects cells from ER stress-induced apoptosis via enhancement of IRE1alpha-XBP1 signaling through a physical interaction. *PLoS Biology, 8*(7), e1000410.

Guzel, A., Er, U., Tatli, M., Aluclu, U., Ozkan, U., & Duzenli, Y., et al. (2008). Serum neuron-specific enolase as a predictor of short-term outcome and its correlation with Glasgow Coma Scale in traumatic brain injury. *Neurosurgical Review*, *31*(4), 439–444; discussion 444–435.

Hamilton, A. J., Trad, L. A., & Cymerman, A. (1991). Alterations in human upper extremity motor function during acute exposure to simulated altitude. *Aviation, Space and Environmental Medicine, 62*(8), 759–764.

Hara, M. R., Cascio, M. B., & Sawa, A. (2006). GAPDH as a sensor of NO stress. *Biochimica et Biophysica Acta, 1762*(5), 502–509.

Harkness, R. A. (1997). Is post-hypoxic-ischemic cell damage associated with excessive ATP consumption rather than a failure of ATP production? *Acta Paediatrica, 86*(1), 1–5.

Hendgen-Cotta, U. B., Merx, M. W., Shiva, S., Schmitz, J., Becher, S., Klare, J. P., et al. (2008). Nitrite reductase activity of myoglobin regulates respiration and cellular viability in myocardial ischemia-reperfusion injury. *Proceedings of National Academy of Science USA, 105*(29), 10256–10261.

Heurteaux, C., Lauritzen, I., Widmann, C., & Lazdunski, M. (1995). Essential role of adenosine, adenosine A1 receptors, and ATP-sensitive K + channels in cerebral ischemic preconditioning. *Proceedings of National Academy of Science USA, 92*(10), 4666–4670.

Hodkinson, P. D. (2011). Acute exposure to altitude. *Journal of the Royal Army Medical Corps, 157*(1), 85–91.

Hong, S. C., Lanzino, G., Goto, Y., Kang, S. K., Schottler, F., Kassell, N. F., et al. (1994). Calcium-activated proteolysis in rat neocortex induced by transient focal ischemia. *Brain Research, 661*(1–2), 43–50.

Indraswari, F., Wong, P. T., Yap, E., Ng, Y. K., & Dheen, S. T. (2009). Upregulation of Dpysl2 and Spna2 gene expression in the rat brain after ischemic stroke. *Neurochemistry International, 55*(4), 235–242.

Janke, C., & Kneussel, M. (2010). Tubulin post-translational modifications: encoding functions on the neuronal microtubule cytoskeleton. *Trends in Neurosciences, 33*(8), 362–372.

Julian, C. G., Subudhi, A. W., Wilson, M. J., Dimmen, A. C., Pecha, T., & Roach, R. C. (2011). Acute mountain sickness, inflammation, and permeability: new insights from a blood biomarker study. *Journal of Applied Physiology, 111*(2), 392–399.

Komarova, Y., Lansbergen, G., Galjart, N., Grosveld, F., Borisy, G. G., & Akhmanova, A. (2005). EB1 and EB3 control CLIP dissociation from the ends of growing microtubules. *Molecular Biology of the Cell, 16*(11), 5334–5345.

Laemmli, U. K. (1970). Cleavage of structural proteins during the assembly of the head of bacteriophage T4. *Nature, 227*(5259), 680–685.

LaManna, J. C., Chavez, J. C., & Pichiule, P. (2004). Structural and functional adaptation to hypoxia in the rat brain. *Journal of Experimental Biology, 207*(Pt 18), 3163–3169.

Lansbergen, G., & Akhmanova, A. (2006). Microtubule plus end: A hub of cellular activities. *Traffic, 7*(5), 499–507.

Lopez-Barneo, J., Pardal, R., & Ortega-Saenz, P. (2001). Cellular mechanism of oxygen sensing. *Annual Review of Physiology, 63*, 259–287.

Lopez-Ramos, J. C., Martinez-Romero, R., Molina, F., Canuelo, A., Martinez-Lara, E., Siles, E., et al. (2005). Evidence of a decrease in nitric oxide-storage molecules following acute hypoxia and/or hypobaria, by means of chemiluminescence analysis. *Nitric Oxide, 13*(1), 62–67.

Maa, E. H. (2010). Hypobaric hypoxic cerebral insults: The neurological consequences of going higher. *NeuroRehabilitation, 26*(1), 73–84.

Martinez-Romero, R., Canuelo, A., Martinez-Lara, E., Hernandez, R., Del Moral, M. L., Pedrosa, J. A., et al. (2006). Aging affects but does not eliminate the enzymatic antioxidative response to hypoxia/reoxygenation in cerebral cortex. *Experimental Gerontology, 41*(1), 25–31.

Martinez-Romero, R., Canuelo, A., Martinez-Lara, E., Javier Oliver, F., Cardenas, S., & Siles, E. (2009). Poly(ADP-ribose) polymerase-1 modulation of in vivo response of brain hypoxia-inducible factor-1 to hypoxia/reoxygenation is mediated by nitric oxide and factor inhibiting HIF. *Journal of Neurochemistry, 111*(1), 150–159.

Martinez-Romero, R., Canuelo, A., Siles, E., Oliver, F. J., & Martinez-Lara, E. (2012). Nitric oxide modulates hypoxia-inducible factor-1 and poly(ADP-ribose) polymerase-1 cross talk in response to hypobaric hypoxia. *Journal of Applied Physiology, 112*(5), 816–823.

Moore, B. W., & McGregor, D. (1965). Chromatographic and electrophoretic fractionation of soluble proteins of brain and liver. *Journal of Biological Chemistry, 240*, 1647–1653.

Morgan, B. L., & Chao, C. R. (2004). The effects of hypoxia on growth cones in the ovine fetal brain. *Journal of Matern Fetal Neonatal Medicine, 16*(1), 55–59.

Morimoto, Y., Kemmotsu, O., & Alojado, E. S. (1997). Extracellular acidosis delays cell death against glucose-oxygen deprivation in neuroblastoma × glioma hybrid cells. *Critical Care Medicine, 25*(5), 841–847.

Nakamura, T., Hinagata, J., Tanaka, T., Imanishi, T., Wada, Y., Kodama, T., et al. (2002). HSP90, HSP70, and GAPDH directly interact with the cytoplasmic domain of macrophage scavenger receptors. *Biochemical and Biophysical Research Communications, 290*(2), 858–864.

Nouette-Gaulain, K., Biais, M., Savineau, J. P., Marthan, R., Mazat, J. P., Letellier, T., et al. (2011). Chronic hypoxia-induced alterations in mitochondrial energy metabolism are not reversible in rat heart ventricles. *Canadian Journal of Physiology and Pharmacology, 89*(1), 58–66.

Opii, W. O., Joshi, G., Head, E., Milgram, N. W., Muggenburg, B. A., Klein, J. B., et al. (2008). Proteomic identification of brain proteins in the canine model of human aging following a long-term treatment with antioxidants and a program of behavioral enrichment: relevance to Alzheimer's disease. *Neurobiology of Aging, 29*(1), 51–70.

Ostergaard, L., Simonsen, U., Eskildsen-Helmond, Y., Vorum, H., Uldbjerg, N., Honore, B., et al. (2009). Proteomics reveals lowering oxygen alters cytoskeletal and endoplasmatic stress proteins in human endothelial cells. *Proteomics, 9*(19), 4457–4467.

Ouyang, Y. B., Xu, L. J., Sun, Y. J., & Giffard, R. G. (2006). Overexpression of inducible heat shock protein 70 and its mutants in astrocytes is associated with maintenance of mitochondrial physiology during glucose deprivation stress. *Cell Stress Chaperones, 11*(2), 180–186.

Pacary, E., Tixier, E., Coulet, F., Roussel, S., Petit, E., & Bernaudin, M. (2007). Crosstalk between HIF-1 and ROCK pathways in neuronal differentiation of mesenchymal stem cells, neurospheres and in PC12 neurite outgrowth. *Molecular and Cellular Neuroscience, 35*(3), 409–423.

Pancholi, V. (2001). Multifunctional alpha-enolase: its role in diseases. *Cellular and Molecular Life Sciences, 58*(7), 902–920.

Pike, B. R., Flint, J., Dave, J. R., Lu, X. C., Wang, K. K., Tortella, F. C., et al. (2004). Accumulation of calpain and caspase-3 proteolytic fragments of brain-derived alphaII-spectrin in cerebral spinal fluid after middle cerebral artery occlusion in rats. *Journal of Cerebral Blood Flow and Metabolism, 24*(1), 98–106.

Planas, A. M., Soriano, M. A., Estrada, A., Sanz, O., Martin, F., & Ferrer, I. (1997). The heat shock stress response after brain lesions: induction of 72 kDa heat shock protein (cell types involved, axonal transport, transcriptional regulation) and protein synthesis inhibition. *Progress in Neurobiology, 51*(6), 607–636.

Raley-Susman, K. M., & Murata, J. (1995). Time course of protein changes following in vitro ischemia in the rat hippocampal slice. *Brain Research, 694*(1–2), 94–102.

Reshef, A., Capua, N. D., Sperling, O., & Zoref-Shani, E. (2000). Ischemic tolerance conferred to cultured rat neurons by heat shock is not mediated by opening of adenosine triphosphate-sensitive potassium channels. *Neuroscience Letters, 287*(3), 223–226.

Rodrigo, J., Fernandez, A. P., Alonso, D., Serrano, J., Fernandez-Vizarra, P., Martinez-Murillo, R., et al. (2004). Nitric oxide in

the rat cerebellum after hypoxia/ischemia. *Cerebellum, 3*(4), 194–203.

Rodrigo, J., Fernandez, A. P., Serrano, J., Peinado, M. A., & Martinez, A. (2005). The role of free radicals in cerebral hypoxia and ischemia. *Free Radical Biology & Medicine, 39*(1), 26–50.

Schmechel, D., Marangos, P. J., & Brightman, M. (1978). Neurone-specific enolase is a molecular marker for peripheral and central neuroendocrine cells. *Nature, 276*(5690), 834–836.

Schwartz, L. M., Smith, S. W., Jones, M. E., & Osborne, B. A. (1993). Do all programmed cell deaths occur via apoptosis? *Proceedings of National Academy of Science USA, 90*(3), 980–984.

Sethy, N. K., Singh, M., Kumar, R., Ilavazhagan, G., & Bhargava, K. (2011). Upregulation of transcription factor NRF2-mediated oxidative stress response pathway in rat brain under short-term chronic hypobaric hypoxia. *Functional & Integrative Genomics, 11*(1), 119–137.

Shen, Y., & Yu, L. C. (2008). Potential protection of curcumin against hypoxia-induced decreases in beta-III tubulin content in rat prefrontal cortical neurons. *Neurochemical Research, 33*(10), 2112–2117.

Sirover, M. A. (2011). On the functional diversity of glyceraldehyde-3-phosphate dehydrogenase: Biochemical mechanisms and regulatory control. *Biochimica et Biophysica Acta, 1810*(8), 741–751.

Sultana, R., Perluigi, M., & Butterfield, D. A. (2006). Protein oxidation and lipid peroxidation in brain of subjects with Alzheimer's disease: Insights into mechanism of neurodegeneration from redox proteomics. *Antioxidants & Redox Signaling, 8*(11–12), 2021–2037.

Sweet, E. S., Previtera, M. L., Fernandez, J. R., Charych, E. I., Tseng, C. Y., Kwon, M., et al. (2011). PSD-95 alters microtubule dynamics via an association with EB3. *Journal of Neuroscience, 31*(3), 1038–1047.

Tavaria, M., Gabriele, T., Kola, I., & Anderson, R. L. (1996). A hitchhiker's guide to the human Hsp70 family. *Cell Stress Chaperones, 1*(1), 23–28.

Taylor, C. T. (2008). Mitochondria and cellular oxygen sensing in the HIF pathway. *Biochemical Journal, 409*(1), 19–26.

Voas, M. G., Lyons, D. A., Naylor, S. G., Arana, N., Rasband, M. N., & Talbot, W. S. (2007). alphaii-spectrin is essential for assembly of the nodes of Ranvier in myelinated axons. *Current Biology, 17*(6), 562–568.

Winkelmann, J. C., & Forget, B. G. (1993). Erythroid and nonerythroid spectrins. *Blood, 81*(12), 3173–3185.

Zhao, J., Sun, S., & Chen, X. (2006). Protective effects of focal ischemic preconditioning and HSP70 expression on middle cerebral artery occlusion in rats. *Journal of Huazhong University of Science and Technology Medicine Science, 26*(4), 436–439.